# Role of Mobile Interstitial Oxygen Atoms in Defect Processes in Oxides: Interconversion between Oxygen-Associated Defects in $SiO_2$ Glass

Koichi Kajihara,[1,*] Linards Skuja,[1,2] Masahiro Hirano,[1] and Hideo Hosono[1,3]

[1]*Transparent Electro-Active Materials Project, ERATO, Japan Science and Technology Agency, KSP C-1232,*
*3-2-1 Sakado Takatsu-ku, Kawasaki 213-0012, Japan*
[2]*Institute of Solid State Physics, University of Latvia, Kengaraga iela 8, LV1063 Riga, Latvia*
[3]*Materials and Structures Laboratory, Tokyo Institute of Technology, 4259 Nagatsuta, Midori-ku, Yokohama 226-8503, Japan*

(Received 18 June 2003; published 9 January 2004)

The role of mobile interstitial oxygen atoms ($O^0$) in defect processes in oxides is demonstrated by interconversion between the oxygen dangling bond and the peroxy radical (POR) in $SiO_2$ glass. Superstoichiometric $O^0$ was created by $F_2$ laser photolysis of the interstitial $O_2$. On annealing above 300 °C, $O^0$ migrated and converted the oxygen dangling bond to POR. Exposure to 5.0 eV light converted POR back to a pair of the oxygen dangling bond and $O^0$ (quantum yield: ~0.1). These findings suggest that various defect processes typically occurring in $SiO_2$ glass at ~300–500 °C are related to migration of $O^0$, which exists in the glass network in the peroxy linkage form.

DOI: 10.1103/PhysRevLett.92.015504 PACS numbers: 61.80.Ba, 61.72.Ji, 76.30.Mi, 82.50.Hp

Silica ($SiO_2$) glass attracts fundamental interest as a model glassy material because of its relative structural simplicity and high purity. Further, it is an outstanding optical material due to its high transparency in the near-infrared to vacuum-ultraviolet spectral regions. While $SiO_2$ glass is by far the most radiation-resistant optical glass, generation of point defects often limits its numerous applications. Similar to many oxides, one of the most typical defects in $SiO_2$ is the oxygen vacancy. While it has been widely studied both theoretically [1,2] and experimentally [3–5], the fate of the other member of the Frenkel pair, the neutral interstitial oxygen atom ($O^0$), has remained poorly understood. This situation is generally similar in other oxides as well [6]. Apart from several theoretical treatments predicting that $O^0$ is relatively strongly bound to the $SiO_2$ network by forming the peroxy linkage ($\equiv\text{Si—O—O—Si}\equiv$) [7–9], there is little experimental evidence on its chemical and spectroscopic properties, due to the absence of distinct spectral fingerprints for $O^0$. There are indications [10] that $O^0$ becomes mobile at around 400 °C, as detected by formation of the interstitial oxygen molecules ($O_2$) at this temperature. Another distinct reaction involving $O^0$ is the formation of the ozone molecules ($O_3$) in $O_2$-rich $SiO_2$ glass [11,12]. Further, it has been proposed in several papers [13–16] that $O^0$ could mediate reactions between the two main oxygen-associated paramagnetic defects in $SiO_2$ glass, the oxygen dangling bonds ($\equiv\text{SiO}^\bullet$, termed "nonbridging oxygen hole centers," NBOHC) and the peroxy radicals ($\equiv\text{SiOO}^\bullet$, POR) [17,18]:

$$\equiv\text{SiO}^\bullet + \text{O}^0 \rightarrow \equiv\text{SiOO}^\bullet, \tag{1a}$$

$$\equiv\text{SiOO}^\bullet \rightarrow \equiv\text{SiO}^\bullet + \text{O}^0. \tag{1b}$$

However, there are no direct experimental data on interaction of $O^0$ with the point defects bound to the $SiO_2$ network, although controversial results have been reported on photolysis of POR: exposure to UV light decomposed PORs via Eq. (1b) [16,19], while exposure to KrF laser light (5.0 eV) destroyed PORs leaving the concentrations of other paramagnetic defects unchanged [20]. This paper presents an experimental confirmation of the role of mobile $O^0$ by demonstrating a reversible conversion between NBOHC and POR in $SiO_2$ glass.

One of the main reasons why the reaction described by Eq. (1a) has remained experimentally unconfirmed is the creation of PORs by another reaction, between the interstitial $O_2$ and the silicon dangling bonds (the $E'$ centers, $\equiv\text{Si}^\bullet$) [21]:

$$\equiv\text{Si}^\bullet + \text{O}_2 \rightarrow \equiv\text{SiOO}^\bullet. \tag{2a}$$

This reaction is generally accepted for the following reasons. First, POR is primarily formed in $O_2$-rich $SiO_2$ glasses [17,22]. Second, thermal anneal bleaches the radiation-induced $E'$ centers and concomitantly creates PORs [17,23]. Third, consistently with the diffusion-limited reaction theory [21,24], an impregnating with additional $O_2$ enhances POR formation [25] while a densification of the glass, which restricts $O_2$ diffusion, suppresses the POR formation [26]. Further, an electron paramagnetic resonance (EPR) study [27] reported a destruction of PORs with x-rays accompanied by a simultaneous creation of the $E'$ centers, suggesting a reverse reaction to Eq. (2a),

$$\equiv\text{SiOO}^\bullet \rightarrow \equiv\text{Si}^\bullet + \text{O}_2. \tag{2b}$$

Evidently, to distinguish the reactions involving $O^0$ [Eqs. (1a) and (1b)] from those involving $O_2$ [Eqs. (2a) and (2b)], the concentrations of $O^0$ and NBOHC must be maximized while those of the $E'$ centers and $O_2$ must be minimized. In the present work, this was implemented by two key techniques using an $F_2$ laser (7.9 eV, 157 nm) to photolyze $O_2$ into $O^0$ [28] and to create NBOHCs [29], and using a photoluminescence (PL) technique to monitor

0031-9007/04/92(1)/015504(4)$20.00

the interstitial $O_2$ in parallel with the measurements of paramagnetic centers.

The sample used was high-purity synthetic $SiO_2$ glass [$(10 \times 6.5 \times 2)$ mm$^3$, SiOH $\sim 2 \times 10^{18}$ cm$^{-3}$]. The amount of the interstitial $O_2$ was set by thermal anneal for 120 h at 900 °C in vacuum ("low-$O_2$" sample) or air ("high-$O_2$" sample). It was below $10^{15}$ cm$^{-3}$ in the low-$O_2$ sample both before and after the vacuum anneal. On the other hand, the air anneal introduced $\sim 5 \times 10^{15}$ cm$^{-3}$ of $O_2$ [30,31], which was measured by the intensity of PL band at 7680 cm$^{-1}$ emitted by the $a^1\Delta_g$ excited state of $O_2$ using a Fourier-transform Raman spectrometer (Model 960, Nicolet) [14]. Excitation was performed via the $b^1\Sigma_g^+$ state by cw 765 nm light from a Ti:$Al_2O_3$ laser (Model Tsunami, Spectra-Physics, $\sim$1 W) [32]. On this setup, $O_2$ concentrations down to $\sim 1 \times 10^{15}$ cm$^{-3}$ could be measured after calibration with $SiO_2$ glass of a known $O_2$ content. The samples were irradiated with an $F_2$ laser (LPF-210, Lambda Physik, pulse duration $\sim$20 ns) with $4.5 \times 10^4$ pulses of $\sim$30 mJ cm$^{-2}$ pulse$^{-1}$ at ambient temperature. Then they were thermally annealed in air to create PORs and subsequently irradiated with a KrF laser (Compex205, Lambda Physik, pulse duration $\sim$20 ns) at ambient temperature to destroy PORs. The concentrations of paramagnetic centers were measured at 77 K by an $X$-band EPR spectrometer (E580, Bruker; microwave power 20 mW and modulation amplitude 0.2 mT for NBOHC and POR; 2 $\mu$W and 0.1 mT for the $E'$ center). The concentrations of the Si-Si bonds were evaluated from their 7.6 eV absorption band measured by a vacuum ultraviolet spectrometer (VU-201M, JASCO).

Exposure to $F_2$ laser light dominantly created the $E'$ centers and NBOHCs (Fig. 1). The concentration of NBOHC exceeded that of the $E'$ center several times. This was explained by creation of pairs of the $E'$ centers and NBOHCs via breaking of the Si-O-Si bonds, supplemented by formation of NBOHCs via photolysis of the SiO-H bonds [29]. The concentration of the laser-induced Si-Si bonds was $\sim 1 \times 10^{15}$ cm$^{-3}$, similar in the low- and high-$O_2$ samples [33]. The interstitial $O_2$ disappeared early during the irradiation, suggesting that $O_2$ was cleaved into a pair of $O^0$ [28].

Thermal conversion of the $F_2$-laser-induced defects was studied by isochronal (10 min) thermal anneals in 100 °C steps from ambient temperature to 800 °C. In the low-$O_2$ sample [Fig. 1(a)], thermal anneal up to 300 °C reduced NBOHC concentration mostly due to reaction with mobile hydrogen [34], while slightly enhancing the $E'$ center concentration. On further raising of temperature, both concentrations of the $E'$ center and NBOHC decreased, whereas that of POR started to grow and peaked at 500 °C. Above 600 °C, all laser-induced defects were annihilated as commonly observed in $SiO_2$ glass. Below 500 °C, $O_2$ was not detectable. However, a measurable amount of $O_2$ emerged at 600 °C, which disappeared at higher temperatures.

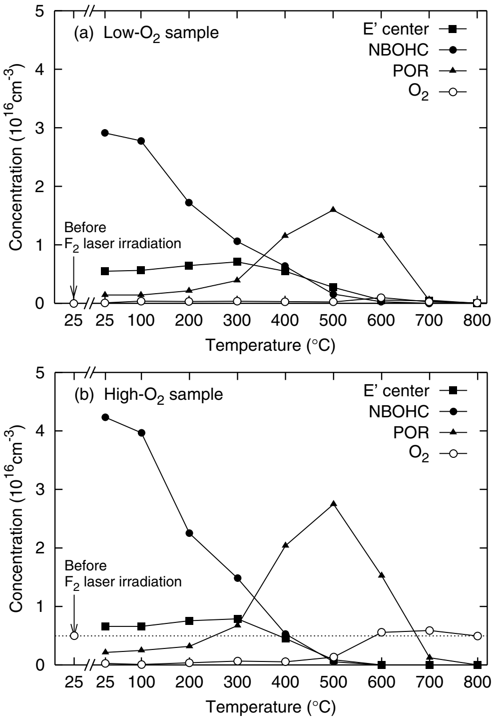

FIG. 1. Concentration changes of the $E'$ center, NBOHC, POR, and interstitial $O_2$ in the $F_2$-laser-irradiated (a) low-$O_2$ and (b) high-$O_2$ samples on isochronal anneals for 10 min at each temperature. In the high-$O_2$ sample, the dotted line indicates the $O_2$ concentration before the irradiation.

Figure 1(b) shows the results for the high-$O_2$ sample. It showed temperature dependences of the paramagnetic defects similar to the case of the low-$O_2$ sample, except for $\sim$1.5 times larger NBOHC and POR concentrations. The interstitial $O_2$, which was destroyed by $F_2$ laser irradiation, started to be restored above 500 °C. It slightly exceeded the preirradiation level at 600 °C and 700 °C, and settled at that level at 800 °C.

The creation of the majority of PORs above 300 °C is unlikely due to Eq. (2a) because of the following reasons. First, the amount of the created PORs was $\sim$3 times larger than that of the destroyed $E'$ centers. Second, the interstitial $O_2$, which should decrease if Eq. (2a) is dominant, remained nearly constant below 500 °C. On the other hand, temperatures at which PORs formed were close to those at which $O^0$ starts migrating to turn into $O_2$ ($\sim$200–400 °C) [10]. Thus, we suggest that most of the PORs were created according to Eq. (1a). However, the decay of the $E'$ center above 300 °C was stronger in the high-$O_2$ sample. It is likely due to a two-step POR formation from the $E'$ center and $O^0$,

$$\equiv\text{Si}^\bullet + 2\text{O}^0 \rightarrow \equiv\text{SiO}^\bullet + \text{O}^0 \rightarrow \equiv\text{SiOO}^\bullet. \qquad (3)$$

The POR concentration in the high-$O_2$ sample was larger than that in the low-$O_2$ sample, indicating that $O_2$ provides $O^0$ to form POR. A significant amount of POR, however, was also found in the low-$O_2$ sample, posing a question on the source of $O^0$ in this case. It is probably not a simple Frenkel process, since the concentration of the laser-induced Si-Si bond was ~10 times lower. Evidently, other $O^0$ sources exist, possibly in the form of the preexisting peroxy linkages [7–9] (see below).

Next, photoconversion of POR to other defects was examined. The $F_2$-laser-irradiated high-$O_2$ sample was thermally annealed at 500 °C in 30 min steps, each followed by KrF laser irradiation (600 pulses of $\sim 100\ \mathrm{mJ\,cm^{-2}\,pulse^{-1}}$) (Fig. 2). In accord with the data of Fig. 1(b), the first thermal anneal step eliminated the $F_2$-laser-induced $E'$ centers and NBOHCs, and enhanced the POR concentration. On the following KrF laser irradiation, the concentration of POR rapidly decreased, while that of NBOHC simultaneously increased, and that of the $E'$ center remained almost unchanged. Similar semireversible concentration changes occurred during the subsequent "anneal-irradiation" cycles. Hence, it is evident that Eq. (1b) controls the KrF-laser-photolysis of POR whereas Eq. (2b) is insignificant. After the first anneal at 500 °C, the $E'$ center concentration remained below $10^{15}\mathrm{cm^{-3}}$ throughout the subsequent anneal-irradiation steps, indicating that POR is created by Eq. (1a) rather than by Eqs. (2a) and (3). On the other hand, $O_2$ accumulated during the anneal-irradiation cycles, indicating that, besides Eq. (1a), $O^0$ is consumed to form $O_2$.

Assuming that Eqs. (1a) and (1b) and the dimerization of $O^0$ are dominant processes in the anneal-irradiation cycles, concentration balances for the paramagnetic centers and excess oxygen species can be given by Eqs. (4a) and (4b), respectively,

$$\Delta[\mathrm{POR}] + \Delta[\mathrm{NBOHC}] = 0, \tag{4a}$$

$$\Delta[\mathrm{POR}] + 2\Delta[O_2] + \Delta[O^0] = 0. \tag{4b}$$

The brackets denote concentration of each species. Equation (4a) qualitatively agrees with the results shown in Fig. 2. However, $|\Delta[\mathrm{NBOHC}]|$ was always smaller than $|\Delta[\mathrm{POR}]|$. This may be in accord with the frequently observed deficiencies in NBOHC concentrations evaluated by EPR compared to those measured by optical absorption, which implies that a part of NBOHCs is EPR silent [16,35]. After a cumulative anneal time of 120 min, the $O_2$ concentration approached the initial level (Fig. 2), making $\Delta[O_2] = 0$ in Eq. (4b). Since KrF laser light hardly cleaves $O_2$, the accumulated $O_2$ is excluded from forming POR via Eq. (1a). Thus, $\Delta[\mathrm{POR}]$ of $\sim 10^{16}\ \mathrm{cm^{-3}}$ is due to $\Delta[O^0]$ that does not originate from the interstitial $O_2$. These $O^0$ probably preexist in the form of less mobile peroxy linkages within a distribution predicted by large site-to-site variations of oxygen binding energies in the peroxy linkage due to structural disorder [9].

The kinetics of KrF-laser-photolysis of POR was examined for the $F_2$-laser-irradiated high-$O_2$ sample that was thermally annealed for 30 min at 500 °C. Figure 3 shows the decay of POR plotted against the number of KrF laser pulses ($n$). Up to ~90% of PORs was bleached within the first 200 pulses ("fast-bleaching POR") while the remaining ~10% survived for $\sim 10^4$ pulses ("slow-bleaching POR") [36]. The decay of the fast-bleaching POR was well fitted with a single exponential, $\exp(-n/\tau)$. The decay rate of POR $(1/\tau)$ depended linearly on the pulse energy (Fig. 3, inset), verifying suggestions [16,19,20] that 5 eV light destroys PORs via one-photon absorption processes. The $E'$ centers were hardly induced during the decay of POR, while the increase of NBOHC concentration followed a single exponential. The formation rate of NBOHC was also proportional to the pulse energy (Fig. 3, inset). Further, it accorded well with the bleaching rate of POR. These findings confirm that 5 eV light decomposes POR by

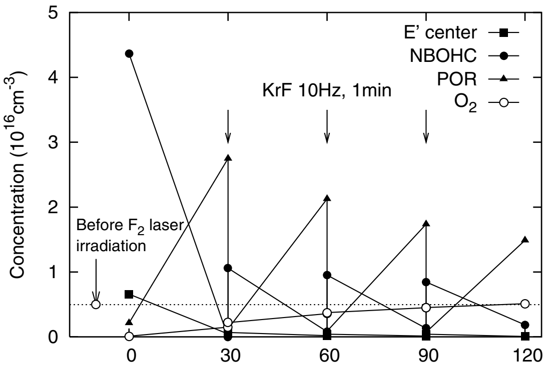

FIG. 2. Concentration changes of the $E'$ center, NBOHC, POR, and interstitial $O_2$ in the $F_2$-laser-irradiated high-$O_2$ sample during multiple cycles of thermal anneal (30 min at 500 °C) and subsequent brief exposure to KrF laser light at ambient temperature (600 pulses of $\sim 100\ \mathrm{mJ\,cm^{-2}\,pulse^{-1}}$). The dotted line indicates the $O_2$ concentration before the $F_2$ laser irradiation.

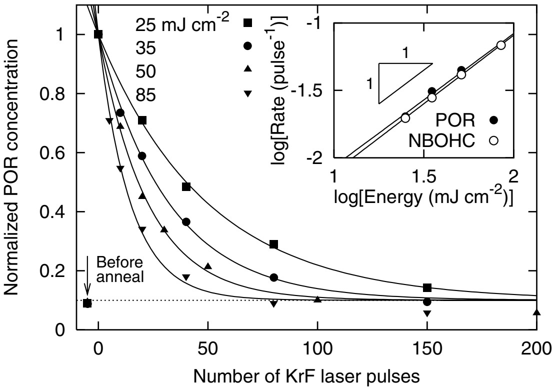

FIG. 3. Normalized concentration change of POR versus number of KrF laser pulses recorded at different pulse energies for the high-$O_2$ sample which has been $F_2$ laser irradiated and thermally annealed for 30 min at 500 °C. The dotted line indicates the POR concentration before the thermal anneal. The inset shows the rates of concentration change of NBOHC and POR as a function of the pulse energy. They were calculated assuming that the concentration change follows a single exponential.

breaking the O-O bond. A study of surface PORs in glassy $SiO_2$ powders reported a similar type photodissociation [19].

The quantum yield of POR photolysis ($\Phi$) was calculated by a relationship,

$$\Phi = 1/(\tau N \sigma), \tag{5}$$

using a $1/(\tau N)$ value ($\sim 6.8 \times 10^{-19}$ $cm^2$), which was obtained from the Fig. 3 inset. Here $N$ is the photon flux of a KrF laser pulse, $\sigma$ is the absorption cross section of POR at 5.0 eV ($\sim 5 \times 10^{-18}$ $cm^2$ [19,37]), and it is assumed that the sample absorption is negligible at 5 eV. This yields $\Phi \sim 0.1$. On the other hand, the photolysis of gaseous organic PORs is mainly due to rupture of the O-O bond which forms the neutral oxygen atom [38], and a $\Phi$ value of ~0.2–0.3 was reported for $CH_3OO^\bullet$ [39]. This similarity of the $\Phi$ values suggests that valence electrons associated with the O-O bond are localized and little influenced by adjacent functional groups, and the oxygen atom released from POR is likely to be neutral.

In summary, this work has demonstrated that diffusion of interstitial oxygen atoms ($O^0$) is a fundamental, thus far largely not explored, mechanism for radiation-induced processes in $SiO_2$ glass. Many thermally activated defect processes in $SiO_2$ take place in the region at ~300–500 °C [13] and the possible influence of oxygen interstitials on these processes must be reevaluated.

---

*Author to whom correspondence should be addressed. Electronic address: k-kajihara@net.ksp.or.jp

[1] E. P. O'Reilly and J. Robertson, Phys. Rev. B **27**, 3780 (1983).
[2] G. Pacchioni and G. Ierano, Phys. Rev. B **57**, 818 (1998).
[3] C. M. Nelson and R. A. Weeks, J. Appl. Phys. **32**, 883 (1961).
[4] H. Hosono, Y. Abe, H. Imagawa, H. Imai, and K. Arai, Phys. Rev. B **44**, 12 043 (1991).
[5] M. Guzzi, M. Martini, A. Paleari, F. Pio, A. Vedda, and C. B. Azzoni, J. Phys. C **5**, 8105 (1993).
[6] E. A. Kotomin and A. I. Popov, Nucl. Instrum. Methods Phys. Res., Sect. B **141**, 1 (1998).
[7] G. Pacchioni and G. Ieranó, Phys. Rev. B **56**, 7304 (1997).
[8] D. R. Hamann, Phys. Rev. Lett. **81**, 3447 (1998).
[9] M. A. Szymanski, A. L. Shluger, and A. M. Stoneham, Phys. Rev. B **63**, 224207 (2001).
[10] L. Skuja, M. Hirano, K. Kajihara, and H. Hosono, Phys. Chem. Glasses **43C**, 145 (2002).
[11] K. Awazu and H. Kawazoe, J. Appl. Phys. **68**, 3584 (1990).
[12] L. Skuja, M. Hirano, and H. Hosono, Phys. Rev. Lett. **84**, 302 (2000).
[13] D. L. Griscom, J. Ceram. Soc. Jpn. **99**, 923 (1991).
[14] L. Skuja and B. Güttler, Phys. Rev. Lett. **77**, 2093 (1996).
[15] D. L. Griscom and M. Mizuguchi, J. Non-Cryst. Solids **239**, 66 (1998).
[16] L. Skuja, M. Hirano, H. Hosono, K. Kajihara, and A. Silin, Glass Sci. Technol.-Glastech. Ber. **75**, 24 (2002).
[17] M. Stapelbroek, D. L. Griscom, E. J. Friebele, and G. H. Sigel, Jr., J. Non-Cryst. Solids **32**, 313 (1979).
[18] E. J. Friebele, D. L. Griscom, M. Stapelbroek, and R. A. Weeks, Phys. Rev. Lett. **42**, 1346 (1979).
[19] V. A. Radzig, in *Defects in* $SiO_2$ *and Related Dielectrics: Science and Technology*, NATO Science Series, edited by G. Pacchioni, L. Skuja, and D. L. Griscom (Kluwer Academic Publishers, Dordrecht, Netherlands, 2000), pp. 339–370.
[20] H. Hosono and R. A. Weeks, J. Non-Cryst. Solids **116**, 289 (1990).
[21] A. H. Edwards and W. B. Fowler, Phys. Rev. B **26**, 6649 (1982).
[22] J. H. Stathis and M. A. Kastner, Phys. Rev. B **29**, 7079 (1984).
[23] T. E. Tsai and D. L. Griscom, Phys. Rev. Lett. **67**, 2517 (1991).
[24] T. R. Waite, Phys. Rev. **107**, 463 (1957).
[25] R. L. Pfeffer, in *The Physics and Technology of Amorphous* $SiO_2$, edited by R. A B. Devine (Plenum, New York, 1988), p. 181.
[26] R. A. B. Devine, J. J. Capponi, and J. Arndt, Phys. Rev. B **35**, 770 (1987).
[27] L. Zhang, V. A. Mashkov, and R. G. Leisure, Phys. Rev. Lett. **74**, 1605 (1995).
[28] L. Skuja, K. Kajihara, T. Kinoshita, M. Hirano, and H. Hosono, Nucl. Instrum. Methods Phys. Res., Sect. B **191**, 127 (2002).
[29] K. Kajihara, Y. Ikuta, M. Hirano, and H. Hosono, Appl. Phys. Lett. **81**, 3164 (2002).
[30] K. Kajihara, T. Miura, H. Kamioka, M. Hirano, L. Skuja, and H. Hosono, J. Non-Cryst. Solids (to be published).
[31] An average value corresponding to $\sim 8 \times 10^{15}$ $cm^{-3}$ at the sample surface and $\sim 3 \times 10^{15}$ $cm^{-3}$ at the center [30].
[32] L. Skuja, B. Güttler, D. Schiel, and A. R. Silin, Phys. Rev. B **58**, 14 296 (1998).
[33] Concentration of the Si-Si bond was calculated using $\sigma$ of $7.3 \times 10^{-17}$ $cm^2$ at 7.6 eV [4].
[34] K. Kajihara, L. Skuja, M. Hirano, and H. Hosono, Phys. Rev. Lett. **89**, 135507 (2002).
[35] If NBOHC is created in a less confined environment, where its dangling oxygen experiences only $C_{3v}$ local field of its own $SiO_4$ tetrahedron, the thermal motion might dynamically degenerate its ground state and render it EPR silent.
[36] These two POR components could be due to different types of PORs: $F_2$-laser-induced POR (Fig. 3, point "before anneal"), whose concentration is notably close to that of the slow-bleaching POR (Fig. 3, point at 200 pulses), might have different configuration from POR created by thermal anneal. The slow-bleaching POR likely has local environment, which hinders the separation of the atomic oxygen after photolysis ("cage effect").
[37] The $\sigma$ value at 5.0 eV was derived from the reported optical absorption parameters of POR ($\sigma$ of $7 \times 10^{-18}$ $cm^2$ at 5.4 eV with full width at half maximum of 1.2 eV) [19].
[38] P. D. Lightfoot, R. A. Cox, J. N. Crowley, M. Destriau, G. D. Hayman, M. E. Jenkin, G. K. Moortgat, and F. Zabel, Atmos. Environ. A **26**, 1805 (1992).
[39] D. Hartmann, J. Karthäuser, and R. Zellner, J. Phys. Chem. **94**, 2963 (1990).